. J. W., *Rec. Trav. Chim.* **60,** 625 (1941).
G. B., MacDonald, L. A., and Redmar,
. Inorg. Nucl. Chem. **6,** 236 (1958).
, and Sen, P. K., *Indian J. Chem.* **12,** 170

H., Salman, T., and Donnay, G., *J. Col-*
terface Sci. **70,** 483 (1979).
, Cooke, S. R. B., and Kim, Y. S., *Trans.*
223, 113 (1962).
, T., and Kittaka, S., *Bull. Chem. Soc.*
46, 3040 (1973).
., *J. Colloid Interface Sci.* **48,** 327 (1974).
W., Hohl, H., and Dalang, F., *Croatica*
Acta **48,** 491 (1976).
ınd Stumm, W., *Colloids and Surf.* **2,** 101

ıi, A. E., Blesa, M. A., and Maroto,
J., Second Argentine Conference of Phys-
hemistry, Córdoba (1980).
ıi, A. E., Figliolia, N. M., Blesa, M. A., and
o, A. J. G., to be published.

Electrostatic Effects on the Partitioning of Spherical Colloids between Dilute Bulk Solution and Cylindrical Pores

FRANK G. SMITH, III[1] AND WILLIAM M. DEEN

Department of Chemical Engineering, Massachusetts Institute of Technology, Cambridge, Massachusetts 02139

Received January 25, 1982; accepted July 7, 1982

Theoretical results are presented for the electrostatic double-layer interaction between a colloid particle and a long cylindrical pore, where the colloid is allowed to assume any radial position within the pore. The colloid particle is represented as a solid sphere with a given surface charge density or surface potential, or as a porous sphere with a given volumetric charge density, and the linear form of the Poisson–Boltzmann equation is employed. Analytical expressions for the potential energy of interaction are obtained and used to calculate equilibrium partitioning coefficients.

INTRODUCTION

Partitioning of solutes between small liquid-filled pores and bulk solution plays a large role in a variety of chromatographic and membrane separation processes. In designing or analyzing such separations it would be desirable to have a predictive theory to relate independently measurable properties of the solute and pore (e.g., size, electrical charge density) to the value of the pore-to-bulk solute concentration ratio at equilibrium, Φ. For the simplest model system, that of a rigid spherical colloid in a cylindrical pore, dilute solution theories of partitioning (1, 2) yield the expression

$$\Phi = C/C_\infty = 2\int_0^{1-\alpha} \exp[-E(\beta)/kT]\beta\, d\beta, \quad [1]$$

where C and C_∞ are average solute concentrations in the pore and bulk solution, respectively, and $E(\beta)/kT$ is the potential energy of interaction between the solute and pore wall, relative to the product of Boltzmann's constant with temperature. In this expression α and β are the sphere radius and a radial coordinate, respectively, both normalized by the pore radius. The upper limit of integration takes into account the fact that the center of a rigid sphere cannot approach the pore wall more closely than one sphere radius; for purely steric interactions ($E = 0$ for $\beta < 1 - \alpha$), Eq. [1] reduces to simply $\Phi = (1 - \alpha)^2$. In the general case the Boltzmann factor involving E is a measure of the probability of finding a solute center at a given radial position β. The same Boltzmann factor appears in expressions describing hindered diffusion and convection of solutes through small pores (1, 2).

In a previous study (3) we developed a model of electrostatic double-layer interactions between spherical colloids and cylindrical pores, to evaluate their contributions to E. That analysis, providing the only available results for this geometry to date, was limited to axisymmetric positions of the spheres and therefore yielded only $E(0)$. Evaluation of the integral in Eq. [1] required assumptions to be made about the approximate radial dependence of E. We present here a generalization of the previous results to include arbitrary radial positions of the solute. As before, two idealized colloid par-

[1] Present address: E. I. DuPont de Nemours & Co., Savannah River Laboratory, Aiken, SC 29808.

Journal of Colloid and Interface Science, Vol. 91, No. 2, February 1983

0021-9797/83/020571-20$03.00/0

ticles are considered, a solid sphere with a uniform surface charge density or surface potential, and a permeable but rigid sphere having a uniform volumetric charge density. The pore is taken to be a rigid circular cylinder essentially infinite in length with either a uniform surface charge density or surface potential. Employing the Gouy–Chapman diffuse double-layer model, an analytical solution to the linearized Poisson–Boltzmann equation is obtained for the electrical potential distribution within the pore. The potential energy of interaction $E(\beta)$ is then calculated from the system free energy using the integral expressions derived by Verwey and Overbeek (4). Use of the linearized equations allows analytical solutions to be obtained for the interaction potential, greatly facilitating application of the theory. The principal results are contained in Eqs. [29], [33], and [37]–[39].

THEORETICAL DEVELOPMENT

The approach is first to obtain general solutions to the linearized Poisson–Boltzmann equation in both cylindrical and spherical coordinates. Boundary conditions on each surface (cylinder or sphere) are then satisfied in their particular coordinate system. This determines some of the unknown coefficients in each infinite series solution. A transformation of one solution into the other coordinate system allows the remaining coefficients to be evaluated. With the electric potential established, the free energy of the system and the interaction potential energy may be determined. In the description that follows, most of the details of the series expansions, coordinate transformation, and other lengthy manipulations have been omitted, together with many intermediate results. The methods used are analogous to those discussed at length in our previous analysis of the axisymmetric problem (3), but their execution in the present three-dimensional case is considerably more involved. The reader interested in a more complete description of the present analysis is referred elsewhere (5).

1. Governing Equations and Boundary Conditions

A solution for the electrical potential is required in both cylindrical (r, ξ, z) and spherical (ρ, ϕ, θ) coordinates. It is found to be convenient to define a set of dimensionless coordinates and parameters using the cylinder radius R_0 as a characteristic length. The dimensionless coordinates, sphere radius (α), and sphere radial position (β), obtained by dividing corresponding dimensional quantities by R_0, are shown in Fig. 1.

The electrical potential ψ^*, cylinder surface charge density q_c, sphere surface charge density q_s, and porous sphere volume charge density q_v are expressed in dimensionless form as

$$\Psi = \frac{F\psi^*}{RT}, \qquad \sigma_c = \frac{FR_0q_c}{\epsilon RT},$$

$$\sigma_s = \frac{FR_0q_s}{\epsilon RT}, \qquad \omega = \frac{FR_0^2q_v}{\epsilon RT\bar{\delta}}.$$

In these relations, F is the Faraday constant, R the gas constant, T the absolute temperature, ϵ the solvent dielectric permittivity and $\bar{\delta}$ the ratio of the sphere dielectric constant to that of the solvent. The dielectric permittivity is defined to be the relative dielectric constant of the medium multiplied by ϵ_0, the permittivity of free space.[2]

The solid material surrounding the pore is assumed to have no net charge beyond that residing on its surface. Accordingly, the electrical potential in this region (Ψ') is governed by Laplace's equation

$$\nabla^2\Psi' = 0. \qquad [2]$$

The linearized Poisson–Boltzmann equation is assumed to describe the electrical potential

[2] As defined here ϵ differs by a factor 4π from that previously used (3). Denoting the previous value by ϵ', $\epsilon = \epsilon'/4\pi$. In the equations presented here $\epsilon_0 = 8.8542 \times 10^{-12}$ C·V^{-1}·m^{-1}.

sent analysis is referred else-

RNING EQUATIONS AND
NDARY CONDITIONS

for the electrical potential is
oth cylindrical (r, ξ, z) and
, θ) coordinates. It is found to
to define a set of dimensionless
ıd parameters using the cylin-
as a characteristic length. The
s coordinates, sphere radius
:e radial position (β), obtained
corresponding dimensional
R_0, are shown in Fig. 1.
cal potential ψ^*, cylinder sur-
ensity q_c, sphere surface charge
d porous sphere volume charge
re expressed in dimensionless

$$\frac{F\psi^*}{RT}, \quad \sigma_c = \frac{FR_0q_c}{\epsilon RT},$$

$$\frac{FR_0q_s}{\epsilon RT}, \quad \omega = \frac{FR_0^2q_v}{\epsilon RT\bar{\delta}}.$$

tions, F is the Faraday constant,
onstant, T the absolute temper-
olvent dielectric permittivity and
of the sphere dielectric constant
e solvent. The dielectric permit-
ıned to be the relative dielectric
the medium multiplied by ϵ_0, the
of free space.[2]
l material surrounding the pore
to have no net charge beyond that
its surface. Accordingly, the elec-
tial in this region (Ψ') is governed
's equation

$$\nabla^2\Psi' = 0. \qquad [2]$$

zed Poisson–Boltzmann equation
to describe the electrical potential

d here ϵ differs by a factor 4π from that
ed (3). Denoting the previous value by ϵ',
the equations presented here $\epsilon_0 = 8.8542$
$^{-1} \cdot m^{-1}$.

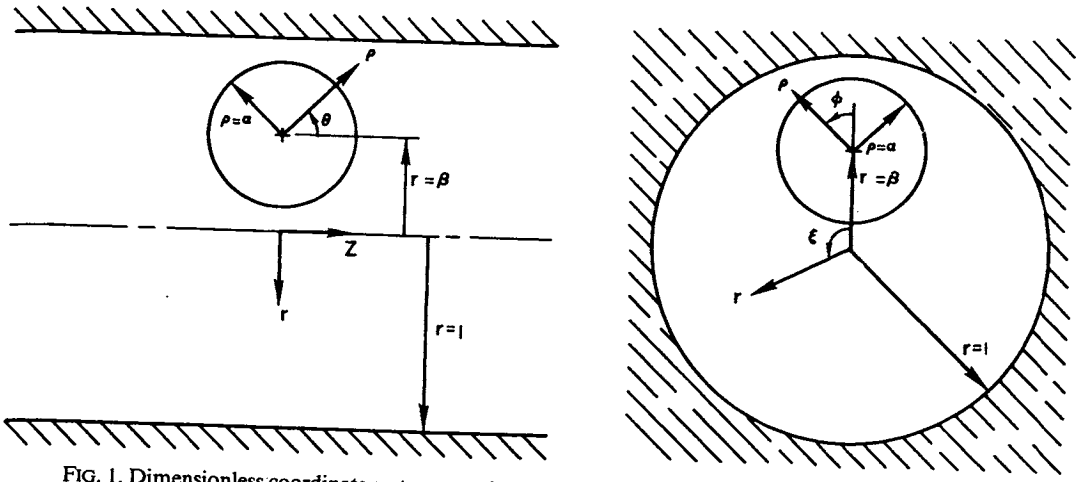

FIG. 1. Dimensionless coordinate systems employed in the theoretical analysis. The sphere and cylinder are shown in both longitudinal cross section (left) and radial cross section (right). The cross-sectional views correspond to the two planes of symmetry in the problem at $z = 0$ or $\theta = \pi/2$ and at $\xi = 0$ or $\phi = 0$.

(Ψ) within the electrolyte solution inside the pore:

$$\nabla^2\Psi = \tau^2\Psi. \qquad [3]$$

The dimensionless parameter τ is the ratio of pore radius to Debye length, given by

$$\tau = R_0\kappa = R_0\left[\frac{F^2}{\epsilon RT}\sum_i (z_i^2c_{i\infty})\right]^{1/2},$$

where $c_{i\infty}$ and z_i are the bulk solution concentration and valence, respectively, of electrolyte species i. Within a solid spherical particle, the electrical potential ($\bar{\Psi}$) is assumed, as with the pore material, to be described by Laplace's equation

$$\nabla^2\bar{\Psi} = 0. \qquad [4]$$

For a porous sphere, the governing equation for the electrical potential is

$$\nabla^2\bar{\Psi} = (\gamma\tau)^2\bar{\Psi} - \omega. \qquad [5]$$

The porous sphere is viewed as a homogeneous structure with an effective dielectric constant ratio $\bar{\delta}$. The parameter γ is defined such that $\bar{\delta}\gamma^2$ is equal to the volume fraction of solvent within the porous sphere. Equation [5] is then derived from the Poisson equation by taking the total charge density within the sphere as the sum of that from the fixed charges (ω) and a contribution from the penetrating electrolyte solution. Consistent with Eq. [3], a linearization of the Boltzmann ion distributions is employed in deriving Eq. [5].

The boundary conditions to be applied for the cylindrical pore at constant surface charge density are:

$$\Psi' \text{ finite} \quad \text{as} \quad r \to \infty, \qquad [6]$$

$$\Psi = \Psi' \quad \text{at} \quad r = 1, \qquad [7a]$$

and

$$\frac{\partial\Psi}{\partial r} - \delta'\frac{\partial\Psi'}{\partial r} = \sigma_c \quad \text{at} \quad r = 1, \qquad [7b]$$

where δ' is the ratio of the dielectric constant of the solid material surrounding the pore to that of the solvent. The boundary conditions for the sphere at constant surface charge density are

$$\bar{\Psi} \text{ finite} \quad \text{at} \quad \rho = 0, \qquad [8]$$

$$\Psi = \bar{\Psi} \quad \text{at} \quad \rho = \alpha, \qquad [9a]$$

and

$$\partial\Psi/\partial\rho - \bar{\delta}\partial\bar{\Psi}/\partial\rho = -\sigma_s \quad \text{at} \quad \rho = \alpha. \qquad [9b]$$

The first boundary condition [6] assumes that the pores are sufficiently well separated that the material surrounding an isolated pore may be viewed as homogeneous and of

infinite extent. Conditions [7a] and [9a] express the continuity of the electrical potential throughout the entire region, while boundary conditions [7b] and [9b] result from an application of Gauss' law of electrostatics at the two surfaces. For the porous sphere, no additional surface charge is assumed to exist, so that $\sigma_s = 0$ in [9b].

When surface potentials are held constant, rather than surface charges, the boundary conditions [7] and [9] are replaced by

$$\Psi = \Psi_c \quad \text{at} \quad r = 1, \qquad [7c]$$

and

$$\Psi = \Psi_s \quad \text{at} \quad \rho = \alpha. \qquad [9c]$$

The electrical potentials within the sphere ($\bar{\Psi}$) and in the material surrounding the pore (Ψ') will be constants in this case and need not be considered in the analysis.

Additionally, as may be seen in Fig. 1, two planes of symmetry defined by the equivalent conditions $z = 0$ or $\theta = \pi/2$ and $\xi = 0$ or $\phi = 0$ exist for this problem. Therefore, the solutions are required to be even in z, ξ, ϕ, and $\theta + \pi/2$. The cylindrical pore is assumed to extend infinitely far in the $\pm z$ directions as viewed from the sphere.

A reference potential value of zero has been taken to exist in the electrolyte solution external to the pore and infinitely far from the charged sphere.

2. Solution for the Electrical Potentials

a. *Solid Sphere Model-Constant Surface Charge Density*

Using the method of separation of variables, general solutions may be written to the basic differential equations for the electrical potentials. Application of this technique to the Helmholtz equation is discussed by Eyges (6) and solutions similar to those found here in cylindrical coordinates have been obtained previously by Karasz and Hill (7).

A solution to Eq. [2] in cylindrical coordinates that is even in z and ξ and that satisfies boundary condition [6] is

$$\Psi'(r, \xi, z) = \frac{\sigma_c I_0(\tau)}{\tau I_1(\tau)} + \sum_{\mu=-\infty}^{\infty} \int_{\lambda'=0}^{\infty} g'_\mu(\lambda') K_\mu(\lambda' r) \cos(\lambda' z) d\lambda' \cos(\mu\xi). \qquad [10]$$

A solution to Eq. [3] in cylindrical coordinates that is even in z and ξ is

$$\Psi(r, \xi, z) = \frac{\sigma_c I_0(\tau r)}{\tau I_1(\tau)} + \sum_{\mu=-\infty}^{\infty} \int_{\lambda=0}^{\infty} \{f_\mu(\lambda) I_\mu[(\tau^2 + \lambda^2)^{1/2} r] + g_\mu(\lambda) K_\mu[(\tau^2 + \lambda^2)^{1/2} r]\} \times \cos(\lambda z) d\lambda \cos(\mu\xi). \qquad [11]$$

In the above equations, I_μ and K_μ are the modified Bessel functions of the first and second kinds, respectively, of order μ and $g'_\mu(\lambda')$, $f_\mu(\lambda)$, and $g_\mu(\lambda)$ represent arbitrary functions of the integration variables that are to be chosen to satisfy the boundary conditions.

The first terms on the right-hand sides of these equations are from the electrical potentials of isolated cylinders and spheres derived elsewhere (3). It may be noted that these terms identically satisfy the boundary conditions [7].

The solution to Eq. [3] in spherical coordinates that is even in ϕ and symmetric about $\theta = \pi/2$ is

$$\Psi(\rho, \phi, \theta) = \sum_{m=0}^{\infty} \sum_{n=0}^{\infty} \left\{ C_{m,2n+m} \left[\frac{p_{2n+m}(-\tau\rho) e^{\tau\rho} - p_{2n+m}(\tau\rho) e^{-\tau\rho}}{(\tau\rho)^{2n+m+1}} \right] + D_{m,2n+m} \frac{p_{2n+m}(\tau\rho) e^{-\tau\rho}}{(\tau\rho)^{2n+m+1}} \right\} \times P^m_{2n+m}(\cos\theta) \cos(m\phi). \qquad [12]$$

The polynomials $p_{2n+m}(\pm\tau\rho)$ are defined by the equation

$$p_{2n+m}(\pm\tau\rho) = \sum_{l=0}^{2n+m} \frac{(2n + m + l)! (\pm\tau\rho)^{2n+m-l}}{2^l l! (2n + m - l)!}$$

$$\frac{\ }{(\tau)} + \sum_{\mu=-\infty}^{\infty} \int_{\lambda'=0}^{\infty}$$

$\lambda' r) \cos(\lambda' z) d\lambda' \cos(\mu\xi)$. [10]

Eq. [3] in cylindrical coordi-
en in z and ξ is

$$\frac{I_0(\tau r)}{I_1(\tau)}$$

$$\int_{\lambda=0}^{\infty} \{f_\mu(\lambda) I_\mu[(\tau^2 + \lambda^2)^{1/2} r]$$

$$_\mu[(\tau^2 + \lambda^2)^{1/2} r]\}$$

$$\times \cos(\lambda z) d\lambda \cos(\mu\xi). \quad [11]$$

equations, I_μ and K_μ are the
sel functions of the first and sec-
respectively, of order μ and
and $g_\mu(\lambda)$ represent arbitrary
the integration variables that are
to satisfy the boundary condi-

erms on the right-hand sides of
ons are from the electrical po-
olated cylinders and spheres de-
here (3). It may be noted that
identically satisfy the boundary
7].
tion to Eq. [3] in spherical coor-
is even in ϕ and symmetric about

$$= \sum_{m=0}^{\infty} \sum_{n=0}^{\infty}$$

$$\left[\frac{p_{2n+m}(-\tau\rho) e^{\tau\rho} - p_{2n+m}(\tau\rho) e^{-\tau\rho}}{(\tau\rho)^{2n+m+1}}\right.$$

$$\left. \cdot m \frac{p_{2n+m}(\tau\rho) e^{-\tau\rho}}{(\tau\rho)^{2n+m+1}}\right\}$$

$$\times P_{2n+m}^m(\cos\theta) \cos(m\phi). \quad [12]$$

nomials $p_{2n+m}(\pm\tau\rho)$ are defined by
ion

$$\rho) = \sum_{l=0}^{2n+m} \frac{(2n+m+l)!(\pm\tau\rho)^{2n+m-l}}{2^l l!(2n+m-l)!}$$

and are found to satisfy the recurrence relations

$$p_k(\pm\tau\rho) = (2k-1) p_{k-1}(\pm\tau\rho) + (\tau\rho)^2 p_{k-2}(\pm\tau\rho) \quad [13]$$

with

$$p_0(\pm\tau\rho) = 1 \quad \text{and} \quad p_1(\pm\tau\rho) = 1 \pm \tau\rho.$$

The P_{2n+m}^m are the associated Legendre polynomials of the first kind of degree $2n + m$ and order m.

The required solution to Eq. [4] in spherical coordinates, having the necessary symmetry in θ and even in ϕ, that satisfies boundary condition [8] is

$$\Psi(\rho, \phi, \theta) = \sum_{m=0}^{\infty} \sum_{n=0}^{\infty} E_{m,2n+m} \times \rho^{2n+m} P_{2n+m}^m(\cos\theta) \cos(m\phi). \quad [14]$$

In Eqs. [12] and [14], $C_{m,2n+m}$, $D_{m,2n+m}$, and $E_{m,2n+m}$ represent constants to be determined from application of the boundary conditions.

The solution procedure is then as follows: (i) Apply boundary conditions [7a] and [7b] to Eqs. [10] and [11], thereby eliminating two of the three arbitrary functions. (ii) Apply boundary conditions [9a] and [9b] to Eqs. [12] and [14] and equate coefficients of like surface harmonics to determine two of the three arbitrary constants involved. (iii) Convert Eq. [11] into spherical coordinates and compare with the form of Eq. [12] to relate the sets of remaining coefficients. The essential idea involved is that, by satisfying one set of boundary conditions with each equation, the known coefficients in one equation correspond to the unknown ones in the other. This procedure generates an infinite set of linear equations that may be solved to obtain as many terms of the electrical potential series representations as desired (5). In establishing these relations the arbitrary functions $g_\mu(\lambda)$ are shown to be of the form

$$g_\mu(\lambda) = \sum_{m=0}^{\infty} \sum_{k=0}^{\infty} a_{m,2k} \lambda^{2k} \eta^m I_{\mu+m}(\eta\beta), \quad [15]$$

where

$$\eta = (\tau^2 + \lambda^2)^{1/2}.$$

Of importance is the fact that the desired interaction energies for this and the other cases to be considered prove to depend only on the coefficients $C_{0,0}$ and $a_{m,0}$ (5). This dependence is shown in Eqs. [28], [32], and [36]. Excellent analytical approximations to these interaction energies (but not the electrical potential itself) can be obtained, as given by Eqs. [29], [33], and [37], by truncating the linear equations governing the coefficients at $m = n = k = 0$. Accordingly, the full set of relations for the coefficients is not given here.

b. Solid Sphere Model-Constant Surface Potential

The solution for the electrolyte electrical potential distribution occurring for a solid sphere and cylinder held at constant surface potentials is constructed in a manner nearly identical to that shown above for the case of constant surface charge densities. Analogous to Eq. [11], a general solution to Eq. [3] in cylindrical coordinates can be written as

$$\Psi(r, \xi, z) = \frac{\Psi_c I_0(\tau r)}{I_0(\tau)} + \sum_{\mu=-\infty}^{\infty} \int_{\lambda=0}^{\infty} \{\hat{f}_\mu(\lambda) I_\mu(\eta r) + \hat{g}_\mu(\lambda) K_\mu(\eta r)\} \cos(\lambda z) d\lambda \cos(\mu\xi). \quad [16]$$

Applying boundary condition [7c] at the cylinder surface eliminates the function $\hat{f}_\mu(\lambda)$. The general solution in spherical coordinates given by Eq. [12] remains unchanged. Applying boundary condition [9c] at the sphere surface, and again equating coefficients of like surface harmonics, generates a set of linear equations relating the coefficients $C_{m,2n+m}$ and $D_{m,2n+m}$. The form of the function $\hat{g}_\mu(\lambda)$ is unchanged from that of $g_\mu(\lambda)$ given in Eq. [15]. Following the transformation of Eq. [16] to spherical coordinates and application of the remaining boundary conditions, an infinite set of linear equations is obtained for the coefficients $a_{m,2k}$, $C_{m,2n+m}$, and $D_{m,2n+m}$. The electrical poten-

tial in the electrolyte solution is then determined using Eq. [12]. The electrical potentials within the sphere and cylinder are simply constants equal to the surface potential values.

c. Porous Sphere Model

For the model of a solvent-permeated sphere having a volumetric charge density ω, a different solution for the electrical potential within the sphere must be employed. A general solution to Eq. [5] in spherical coordinates that satisfies boundary condition [8] and that has the required angular symmetry is given by

$$\bar{\Psi}(\rho, \phi, \theta) = \frac{\omega}{(\gamma\tau)^2} + \sum_{m=0}^{\infty}\sum_{n=0}^{\infty} H_{m,2n+m} \times \left[\frac{p_{2n+m}(-\gamma\tau\rho)e^{\gamma\tau\rho} - p_{2n+m}(\gamma\tau\rho)e^{-\gamma\tau\rho}}{(\gamma\tau\rho)^{2n+m+1}}\right] \times p^m_{2n+m}(\cos\theta)\cos(m\phi). \quad [17]$$

The polynomials $p_{2n+m}(\pm\gamma\tau\rho)$ satisfy a recurrence relation identical to that of Eq. [13]. The expression for $\bar{\Psi}$ in Eq. [17] replaces that of Eq. [14] for the solid sphere analysis. The calculation then proceeds exactly as for the solid sphere model at constant surface charge densities. In using Eq. [17] to satisfy the sphere boundary conditions [9], $\sigma_s = 0$ in this case. The analysis results in an infinite set of linear equations relating the coefficients $C_{m,2n+m}$, $D_{m,2n+m}$, $H_{m,2n+m}$, and $a_{m,2k}$ (5).

Considering the limiting case of a completely porous sphere leads to a significant simplification of the above results. By a completely porous sphere is meant one that is so permeated with solvent that it can be given a porosity of unity and assumed to have the dielectric constant of the solvent. This sets the two parameters $\bar{\delta}$ and γ to unity. Introducing these values into the set of linear equations referred to above, it is possible to show that

$$a_{0,0} = \frac{\omega}{\pi\tau^3}[(1+\tau\alpha)e^{-\tau\alpha} - (1-\tau\alpha)e^{\tau\alpha}] \quad [18]$$

and $a_{m,2k} = 0$ for $m \neq 0$ or $k \neq 0$. It may then be shown that, for this case, the electrical potential both within the sphere and throughout the electrolyte solution can be written compactly as

$$\Psi(\rho, \phi, \theta) = \sum_{m=0}^{\infty}\sum_{n=0}^{\infty} C_{m,2n+m}\left[\frac{p_{2n+m}(-\tau\rho)e^{\tau\rho} - p_{2n+m}(\tau\rho)e^{-\tau\rho}}{(\tau\rho)^{2n+m+1}}\right]P^m_{2n+m}(\cos\theta) \times \cos(m\phi) + \frac{\omega}{2\tau^3\rho}\begin{cases}2\tau\rho - (1+\tau\alpha)e^{-\tau\alpha}(e^{\tau\rho} - e^{-\tau\rho}), & 0 \le \rho \le \alpha \\ [(1+\tau\alpha)e^{-\tau\alpha} - (1-\tau\alpha)e^{\tau\alpha}]e^{-\tau\rho}, & \alpha \le \rho.\end{cases} \quad [19]$$

The major simplification for the completely porous sphere is that the coefficients $C_{m,2n+m}$ appearing in Eq. [19] can be determined without solving a large set of linear equations. The relations governing these coefficients are given elsewhere (5).

3. Free Energy and Interaction Potential Energy

a. Calculation of Free Energy from Electrical Potential

The potential energy for electrostatic double-layer interaction is obtained as the change in free energy on forming the system. That is, the potential is equal to the difference between the free energy of the sphere–cylinder system and that of the individual sphere and cylinder when at infinite separation. It is convenient to define a dimensionless excess free energy G from its dimensional counterpart G^* as

$$G = (F/RT)^2 G^*/\epsilon R_0. \quad [20]$$

As discussed previously (3), with the linearized Poisson–Boltzmann equation employed here the general expressions for electrostatic free energy given by Verwey and Overbeek

or the solid sphere analysis. The then proceeds exactly as for the model at constant surface charge using Eq. [17] to satisfy the dary conditions [9], $\sigma_s = 0$ in this alysis results in an infinite set of ations relating the coefficients $_{,2n+m}$, $H_{m,2n+m}$, and $a_{m,2k}$ (5). ing the limiting case of a com- ous sphere leads to a significant on of the above results. By a com- ous sphere is meant one that is so with solvent that it can be given of unity and assumed to have the onstant of the solvent. This sets rameters $\bar{\delta}$ and γ to unity. Intro- se values into the set of linear referred to above, it is possible to

$$[(1 + \tau\alpha)e^{-\tau\alpha} - (1 - \tau\alpha)e^{\tau\alpha}] \quad [18]$$

= 0 for $m \neq 0$ or $k \neq 0$. It may then that, for this case, the electri- tial both within the sphere and it the electrolyte solution can be mpactly as

$$\left.\begin{array}{l} \left.-\right]P^m_{2n+m}(\cos\theta) \\ {}^{-\tau\alpha}(e^{\tau\rho} - e^{-\tau\rho}), \quad 0 \le \rho \le \alpha \\ 1 - \tau\alpha)e^{\tau\alpha}]e^{-\tau\rho}, \quad \alpha \le \rho. \end{array}\right. \quad [19]$$

ergy on forming the system. That tential is equal to the difference be- free energy of the sphere–cylinder d that of the individual sphere and when at infinite separation. It is con- o define a dimensionless excess free from its dimensional counterpart

$$G = (F/RT)^2 G^*/\epsilon R_0. \quad [20]$$

ssed previously (3), with the linear- son–Boltzmann equation employed general expressions for electrostatic rgy given by Verwey and Overbeek (4) reduce to surface integrals of potential or charge density. For solid surfaces at constant charge density:

$$G^\sigma = \frac{\sigma}{2}\int_A \Psi(\sigma)dA, \quad [21]$$

where A denotes the area of the surface. For solid surfaces at constant surface potential

$$G^\Psi = -\frac{\Psi}{2}\int_A \sigma(\Psi)dA. \quad [22]$$

For the porous sphere, the general expression of Tanford (8) reduces to

$$G^\omega = \frac{\omega}{2}\int_V \Psi(\omega)dV, \quad [23]$$

where the integration is now over the volume V of the porous sphere.

The desired free energy changes are expressed as

$$\Delta G^\sigma = G^\sigma_{sc} - G^\sigma_s - G^\sigma_c, \quad [24]$$

$$\Delta G^\psi = G^\psi_{sc} - G^\psi_s - G^\psi_c, \quad [25]$$

$$\Delta G^\omega = G^\omega_{sc} - G^\omega_s - G^\omega_c, \quad [26]$$

where the subscripts s, c and sc denote the isolated sphere, isolated cylinder (pore), and the combined (interacting) sphere and cylinder, respectively. The various free energy terms for isolated spheres or pores are readily evaluated and have been given previously (3). Free energy calculations for the three composite systems are outlined below.

b. Solid Sphere Model-Constant Surface Charge Density

The free energy of the composite system may be calculated for this model from the formula

$$G^\sigma_{sc} = \frac{\alpha^2\sigma_s}{2}\int_{\phi=0}^{2\pi}\int_{\theta=0}^{\pi}\Psi(\rho,\phi,\theta)|_{\rho=\alpha}\sin\theta d\theta d\phi + \sigma_c\int_{z=0}^{L/2}\int_{\xi=0}^{2\pi}\Psi(r,\xi,z)|_{r=1}d\xi dz, \quad [27]$$

where L is the length of the pore.

The electrical potential $\Psi(\rho, \phi, \theta)$ required for the first integral of Eq. [27] is that given in Eq. [12] evaluated at $\rho = \alpha$, the sphere surface. The angular integrations are performed by using the orthogonality properties of the associated Legendre polynomials and $\cos(m\phi)$. The second integral of Eq. [27], covering the surface of the pore, is evaluated in the limit $L/2 \to \infty$ using the expression for the electrical potential $\Psi(r, \xi, z)$ given in Eq. [11]. Details of these integrations are given elsewhere (5). The resulting expression for the interaction energy is

$$\Delta G^\sigma = \frac{4\pi\alpha^2 e^{\tau\alpha}\sigma_s}{(1+\tau\alpha)}C_{0,0} + \frac{\pi^2\sigma_c}{\tau I_1(\tau)}\sum_{m=0}^{\infty}a_{m,0}\tau^m I_m(\tau\beta). \quad [28]$$

For the axisymmetric case of $\beta = 0$ the only contribution to the final term will occur for $m = 0$, giving a result in agreement with that obtained previously (3).

Numerical calculations performed with the equations governing $C_{0,0}$ and $a_{m,0}$ (5) indicate that an excellent approximation to the exact solution for the interaction potentials is obtained by retaining only the first (all coefficient indices = 0) set of linear equations in the procedure (see Results and Discussion). Similar to the technique employed with the completely porous sphere, the coefficients $C_{0,0}$ and $a_{0,0}$ appearing in the interaction potential equations may then be solved for explicitly. The resulting simplified formulas greatly reduce the computational effort required. The result corresponding to Eq. [28] is

$$\Delta G^\sigma = \frac{\{[8\pi\tau\alpha^4 e^{\tau\alpha}/(1+\tau\alpha)^2]\Delta\sigma_s^2 + [4\pi^2\alpha^2 I_0(\tau\beta)/(1+\tau\alpha)I_1(\tau)]\sigma_s\sigma_c + [\pi I_0(\tau\beta)/\tau I_1(\tau)]^2[(e^{\tau\alpha} - e^{-\tau\alpha})\tau\alpha L(\tau\alpha)/(1+\tau\alpha)]\sigma_c^2\}}{\pi\tau e^{-\tau\alpha} - 2(e^{\tau\alpha} - e^{-\tau\alpha})\tau\alpha L(\tau\alpha)\Delta/(1+\tau\alpha)}, \quad [29]$$

where $L(\tau\alpha)$ indicates the Langevin function $L(\tau\alpha) = \coth(\tau\alpha) - 1/\tau\alpha$. Equation [29] clearly illustrates the quadratic dependence of the interaction potential on the charge densities of the sphere and cylinder (σ_s and σ_c, respectively). For small values of δ', the ratio of the dielectric constant of the material surrounding the pore to that of the solvent, the function Λ is well represented by (5)

$$\Lambda \cong \frac{\pi}{2} I_0(\tau\beta) \sum_{t=0}^{\infty} \frac{\beta^t (2t)!}{2^{3t}(t!)^2} I_t(\tau\beta) \times \left[\tau K_{t+1}(2\tau) + \frac{C}{4} K_t(2\tau)\right], \quad [30]$$

where $K_{t+1}(2\tau)$ and $K_t(2\tau)$ are the modified Bessel functions of the second kind of order $t+1$ and t, respectively. The constant C is equal to 3 for Λ and to -1 for Λ' (see Eq. [33]) which otherwise is identical. In aqueous systems typically $\delta' \cong 0.05$, and for the axisymmetric case use of the equivalent approximation has previously been shown to give excellent results (3). The nature of the approximations required in deriving Eq. [30] is discussed more completely by Smith (5).

c. *Solid Sphere Model-Constant Surface Potential*

The free energy of the sphere–cylinder system for interaction at constant surface potentials is

$$G_{sc}^{\Psi} = -\frac{\alpha^2 \Psi_s}{2} \int_{\phi=0}^{2\pi} \int_{\theta=0}^{\pi} \sigma(\rho, \phi, \theta)|_{\rho=\alpha} \sin\theta d\theta d\phi - \Psi_c \int_{z=0}^{L/2} \int_{\xi=0}^{2\pi} \sigma(r, \xi, z)|_{r=1} d\xi dz. \quad [31]$$

The surface charge densities in the integrals are determined from the electrical potential gradients by applying Gauss' Law. Performing the integration in a manner similar to the constant charge case, and subtracting the free energy contributions of the isolated sphere and cylinder yields

$$\Delta G^{\Psi} = 4\pi\alpha e^{\tau\alpha} \Psi_s C_{0,0} + \frac{\pi^2 \Psi_c}{I_0(\tau)} \sum_{m=0}^{\infty} a_{m,0} \tau^m I_m(\tau\beta). \quad [32]$$

The result in Eq. [32] correctly reduces to the previous axisymmetric solution (3) for $\beta = 0$. Truncating the set of linear equations governing $C_{0,0}$ and $a_{m,0}$ again provides an excellent approximation to the exact solution. The result is

$$\Delta G^{\psi} = \frac{-[8\pi\tau\alpha^2 e^{\tau\alpha}\Lambda']\Psi_s^2 + [4\pi^2\tau\alpha(I_0(\tau\beta)/I_0(\tau))]\Psi_s\Psi_c - [\pi I_0(\tau\beta)/I_0(\tau)]^2(e^{\tau\alpha} - e^{-\tau\alpha})\Psi_c^2}{\pi\tau e^{-\tau\alpha} - 2(e^{\tau\alpha} - e^{-\tau\alpha})\Lambda'}, \quad [33]$$

where Λ' is evaluated from Eq. [30] with $C = -1$. Equation [33] can be placed in the same form as the constant charge result by relating the given surface potentials to the corresponding charge densities at infinite separation. Denoting these charge densities at infinite separation by $\sigma_{s\infty}$ (sphere) and $\sigma_{c\infty}$ (cylinder) the relations are (3): $\Psi_s = \alpha\sigma_{s\infty}/(1+\tau\alpha)$ and $\Psi_c = \sigma_{c\infty} I_0(\tau)/\tau I_1(\tau)$. Equation [33] is then converted into the entirely equivalent form

$$\Delta G^{\Psi} = \frac{-[(8\pi\tau\alpha^4 e^{\tau\alpha}/(1+\tau\alpha)^2)\Lambda']\sigma_{s\infty}^2 + [4\pi^2\alpha^2 I_0(\tau\beta)/(1+\tau\alpha)I_1(\tau)]\sigma_{s\infty}\sigma_{c\infty} - [\pi I_0(\tau\beta)/\tau I_1(\tau)]^2(e^{\tau\alpha} - e^{-\tau\alpha})\sigma_{c\infty}^2}{\pi\tau e^{-\tau\alpha} - 2(e^{\tau\alpha} - e^{-\tau\alpha})\Lambda'}. \quad [34]$$

Equation [34] is seen to be nearly identical to Eq. [29]. The main difference between the two results is a change in sign for the terms involving the squared sphere and cylinder charge

$\sigma_{c\infty} = \frac{\Psi_c \tau I_1(\tau)}{I_0(\tau)}$ $\sigma_{s\infty} = \frac{\Psi_s (1+\tau\alpha)}{\alpha}$

densities. The significance of this difference between the constant charge and constant potential interactions is discussed below.

d. Porous Sphere Model

The free energy formula for this system is

$$G_{sc}^{\omega} = \frac{\omega}{2}\int_{\rho=0}^{\alpha}\int_{\phi=0}^{2\pi}\int_{\theta=0}^{\pi}\bar{\Psi}(\rho,\phi,\theta)\rho^2\sin\theta\,d\theta\,d\phi\,d\rho + \sigma_c\int_{z=0}^{L/2}\int_{\xi=0}^{2\pi}\Psi(r,\xi,z)|_{r=1}d\xi dz. \quad [35]$$

Performing the indicated volume and surface integrations and combining the results with those for the isolated sphere and cylinder gives the exact relation

$$\Delta G^{\omega} = \frac{\pi^2\sigma_c}{\tau I_1(\tau)}\sum_{m=0}^{\infty}a_{m,0}\tau^m I_m(\tau\beta) + \frac{4\pi\alpha e^{\tau\alpha}\omega}{(\gamma\tau)^2}\left[\frac{(1+\gamma\tau\alpha)e^{-\gamma\tau\alpha}-(1-\gamma\tau\alpha)e^{\gamma\tau\alpha}}{[1+\tau\alpha-\bar{\delta}(1-\gamma\tau\alpha)]e^{\gamma\tau\alpha}-[1+\tau\alpha-\bar{\delta}(1+\gamma\tau\alpha)]e^{-\gamma\tau\alpha}}\right]C_{0,0}. \quad [36]$$

The approximation to Eq. [36] obtained by truncating the linear equations governing the coefficients is

$$\Delta G^{\omega} = \left[\frac{8\pi\tau\alpha^2e^{\tau\alpha}\Lambda}{(\gamma\tau)^4\bar{\delta}[1+(1+\tau\alpha)/\bar{\delta}\gamma\tau\alpha L(\gamma\tau\alpha)]^2}\right]\omega^2 + \left[\frac{2\pi^2\alpha(1+\bar{\delta})I_0(\tau\beta)}{(\gamma\tau)^2\bar{\delta}I_1(\tau)[1+(1+\tau\alpha)/\bar{\delta}\gamma\tau\alpha L(\gamma\tau\alpha)]}\right]\omega\sigma^c + \frac{+[\pi I_0(\tau\beta)/\tau I_1(\tau)]^2(e^{\tau\alpha}-e^{-\tau\alpha})\tau\alpha[(L(\tau\alpha)-\bar{\delta}\gamma L(\gamma\tau\alpha))/(1+\tau\alpha+\bar{\delta}\gamma\tau\alpha L(\gamma\tau\alpha))]\sigma_c^2}{\pi\tau e^{-\tau\alpha}-2(e^{\tau\alpha}-e^{-\tau\alpha})\tau\alpha[(L(\tau\alpha)-\bar{\delta}\gamma L(\gamma\tau\alpha))/(1+\tau\alpha+\bar{\delta}\gamma\tau\alpha L(\gamma\tau\alpha))]\Lambda}. \quad [37]$$

Although a more complicated expression has resulted than for the solid sphere cases, with an evaluation of Λ, using Eq. [30] it is possible to readily calculate the interaction potential.

A simplified version of Eq. [36] is possible for the special case of the completely porous sphere, $\gamma = 1$ and $\bar{\delta} = 1$. As given in Eq. [18], $a_{0,0}$ is now the only nonvanishing coefficient in the summation, and an explicit expression for $C_{0,0}$ is also obtainable without resorting to solution of a set of linear equations. The relatively simple result is

$$\Delta G^{\omega} = \frac{2\pi\alpha(e^{\tau\alpha}-e^{-\tau\alpha})L(\tau\alpha)}{\tau^2}\times\left[\frac{I_0(\tau\beta)\sigma_c}{\tau I_1(\tau)} + \frac{\alpha(e^{\tau\alpha}-e^{-\tau\alpha})L(\tau\alpha)}{\pi\tau^2}\Lambda\omega\right]\omega. \quad [38]$$

Equation [38] may be obtained directly from Eq. [37] by setting $\bar{\delta} = \gamma = 1$. It may be noted from Eq. [38] that $\Delta G^{\omega} = 0$ when $\omega = 0$ so that, as expected, there is no interaction energy associated with an uncharged sphere of unit porosity. As with the solid sphere results, the above relations for the porous sphere model reduce for $\beta = 0$ to the previously reported axisymmetric expressions (3).

Finally, Eq. [20] indicates that the dimensional interaction energy $E(\beta)$ in Eq. [1] is related to the dimensionless quantities ΔG by

$$E(\beta) = R_0\epsilon(RT/F)^2\Delta G. \quad [39]$$

For practical calculations ΔG may be evaluated from Eq. [29], [33], [37], or [38], according to the model chosen. Values of the equilibrium partitioning coefficient Φ may then be obtained by numerical integration of Eq. [1]. In the results presented here a

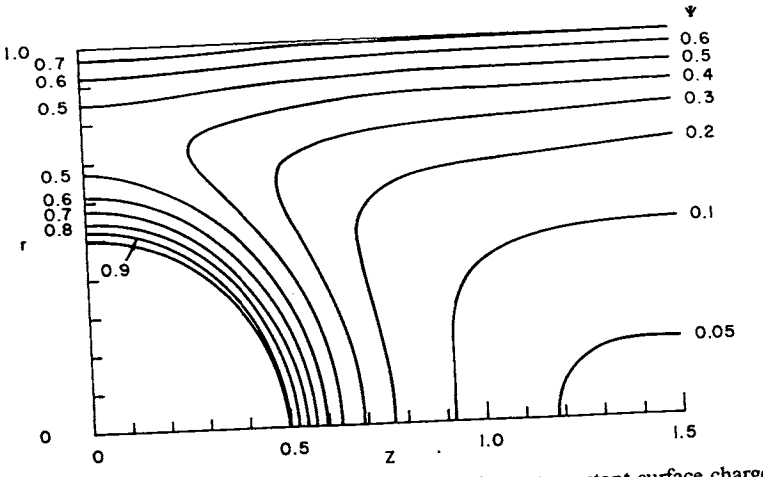

FIG. 2. Equipotential surfaces for an axisymmetric solid sphere at constant surface charge density in a 0.02 M aqueous solution of a 1:1 univalent electrolyte. Parameter values in the calculation are: R_0 = 10 nm, $\alpha = 0.50$, $q_c = 5 \times 10^{-3}$ C·m^{-2}, $q_s = 1 \times 10^{-2}$ C·m^{-2}, and $T = 37$°C, with the surface charges of like sign. Calculations are based on Eq. [12] with $m = 0$ and six terms in the remaining series retained. The series coefficients are evaluated as described previously (3).

Simpson's rule integration was used, generally with the integral evaluated using 100 and then 200 points, and an improved estimate of the partition coefficient obtained by extrapolation.

RESULTS AND DISCUSSION

The electrostatic contributions to the interaction energy $E(\beta)$ reflect distortions in the electrical potentials near the colloid particle (caused by the pore) and near the pore wall (caused by the particle). Equipotential surfaces for a representative case are shown in Fig. 2, to illustrate these effects. Calculations are based on the solid sphere model at constant charge density, with the axisymmetric case ($\beta = 0$) being shown for simplicity. Near the particle the potential attempts to behave like that around an isolated sphere, where equipotential surfaces are concentric spheres. Similarly, near the pore wall and far from the sphere the field appears more like that of an isolated cylinder, where equipotential surfaces are concentric cylinders (parallel lines in Fig. 2). For the isolated sphere and cylinder under these conditions, the dimensionless surface potentials would be uniform at the values $\Psi_{s\infty} = 0.869$ and $\Psi_{c\infty} = 0.686$, respectively, and the cylinder centerline potential would be 0.033. As expected, Fig. 2 shows the greatest deviations of surface potentials at the point of closest approach of the charged surfaces.

For sphere positions other than on the cylinder axis ($\beta \neq 0$), the complicated functional dependence has limited our determination of the electrical potential to evaluation of the first few terms in the series solutions (5). However, as shown in Eqs. [28], [32], and [36], the interaction energies needed for equilibrium partitioning calculations depend only upon certain leading coefficients ($C_{0,0}$ and $a_{m,0}$) of the infinite series. Moreover, the series involving the coefficients $a_{m,0}$ appear to converge very quickly. As illustrated for the solid sphere model in Table I, the second and third terms in the series of Eq. [28] are much smaller than the first, indicating that the sum may be well represented by the first term, $a_{0,0} I_0(\tau\beta)$. Accordingly, to calculate ΔG^σ, $C_{0,0}$ and $a_{0,0}$ are the only coefficients needed to be known accurately. The adequacy of the approximate expression for ΔG^σ, Eq. [29], may be judged from the partition coefficient results shown in Table II. Results from Eq. [29] are compared here with those from Eq.

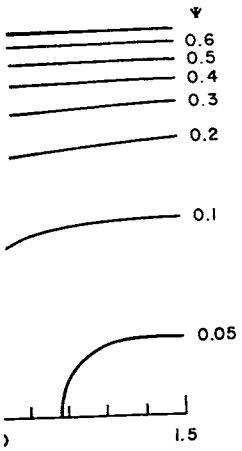

re at constant surface charge density in meter values in the calculation are: R_0 , and $T = 37°C$, with the surface charges ix terms in the remaining series retained.

vely, and the cylinder centerline po- vould be 0.033. As expected, Fig. 2 ne greatest deviations of surface po- at the point of closest approach of ged surfaces.

here positions other than on the cyl- is ($\beta \neq 0$), the complicated functional ence has limited our determination lectrical potential to evaluation of the v terms in the series solutions (5). er, as shown in Eqs. [28], [32], and e interaction energies needed for equi- partitioning calculations depend only ertain leading coefficients ($C_{0,0}$ and the infinite series. Moreover, the se- olving the coefficients $a_{m,0}$ appear to ge very quickly. As illustrated for the here model in Table I, the second and rms in the series of Eq. [28] are much r than the first, indicating that the sum e well represented by the first term, $\tau\beta$). Accordingly, to calculate ΔG^σ, $C_{0,0}$ $_{,0}$ are the only coefficients needed to own accurately. The adequacy of the kimate expression for ΔG^σ, Eq. [29], e judged from the partition coefficient ; shown in Table II. Results from Eq. re compared here with those from Eq. [28], where in the latter $C_{0,0}$ and $a_{m,0}$ were obtained by numerical solution of the appropriate set of linear equations to determine the first four coefficients in each series (5). It can be seen that the results from Eq. [29], which are relatively easy to compute, provide an excellent approximation to the more exact values obtained with Eq. [28]. Since in deriving Eq. [29] $C_{0,0}$ and $a_{0,0}$ were evaluated by truncating the linear equations beyond coefficient indices of zero, this indicates that these two leading coefficients are relatively insensitive to the higher-order terms. All other calculations of Φ presented here are therefore based on the approximate expressions for ΔG, Eqs. [29], [33], [37], and [38].

Figure 3 shows a calculation of partition coefficients for solid spheres of varying size within a 50-nm pore, at several levels of the electrolyte concentration. Interaction is assumed to occur at the constant surface charge densities indicated. The charge on the sphere is taken to be of the same sign as that on the cylinder wall and, therefore, a repulsive electrostatic interaction is observed, decreasing the partition coefficient. For reference, the partition coefficient for neutral hard spheres within neutral pores, $\Phi = (1 - \alpha)^2$, is also plotted. With electrostatic effects absent, the partitioning is solely a steric effect of the hard sphere interaction. The neutral curve would also apply for the limiting case of an infinite solution ionic strength. As the ionic strength is decreased, the two double layers interact more strongly and the partition coefficient decreases. The electrostatic interaction is found to be quite significant at low ionic strength even for the moderate charge levels assumed in this calculation. Thus at an α value of 0.3 the partition coefficient at 0.005 M electrolyte is decreased by an order of magnitude below the neutral or high ionic strength value.

The results just discussed are based on a fixed pore radius (50 nm) with variations in α being due to different particle sizes. If a smaller pore radius is chosen, with the same charge densities, electrolyte concentration, and relative particle size (α), partition coefficients are less in the smaller pore. This may be explained qualitatively by recognizing that at a given ionic strength, the Debye length is a fixed value. However, in the smaller pore, for a given α, this length is larger relative to the sphere and cylinder radii. This leads to greater double-layer "overlap" and therefore a stronger electrostatic interaction is observed in the calculations.

A comparison between alternative models of the solute particle, solid or porous sphere,

TABLE I

Convergence of the Series in Eq. [28][a]

τ	β	$\frac{a_{1,0}\tau I_1(\tau\beta)}{a_{0,0}I_0(\tau\beta)}$	$\frac{a_{2,0}\tau^2 I_2(\tau\beta)}{a_{0,0}I_0(\tau\beta)}$
2	0.1	4.874×10^{-6}	1.050×10^{-10}
2	0.4	8.453×10^{-5}	2.808×10^{-8}
2	0.7	3.236×10^{-4}	3.027×10^{-7}
6	0.1	2.439×10^{-5}	2.524×10^{-8}
6	0.4	4.881×10^{-4}	5.691×10^{-6}
6	0.7	3.665×10^{-3}	8.161×10^{-5}
10	0.1	7.223×10^{-6}	4.739×10^{-8}
10	0.4	2.436×10^{-4}	1.202×10^{-5}
10	0.7	5.016×10^{-3}	3.652×10^{-4}

[a] Calculations are for a solid sphere at constant surface charge density in a 1:1 univalent electrolyte solution at 37°C with $R_0 = 20$ nm, $\alpha = 0.20$, $q_s = q_c = 10^{-2}$ C·m^{-2}, $\bar{\delta} = 0.10$, and $\delta' = 0$.

TABLE II

Partition Coefficient Calculations[a]

τ	ϕ (Eq. 28)	ϕ (Eq. 29)	Percentage error
2.097	5.826×10^{-34}	5.323×10^{-34}	8.63
4.690	7.853×10^{-4}	7.512×10^{-4}	4.34
6.632	5.229×10^{-2}	5.143×10^{-2}	1.64
9.379	1.987×10^{-1}	1.980×10^{-1}	0.35
20.97	4.670×10^{-1}	4.462×10^{-1}	4.45

[a] Calculations are for a solid sphere at constant surface charge density in a 1:1 univalent electrolyte solution at 37°C with $R_0 = 20$ nm, $\alpha = 0.25$, $q_s = q_c = 10^{-2}$ C·m^{-2}, $\bar{\delta} = 0.1$, and $\delta' = 0$.

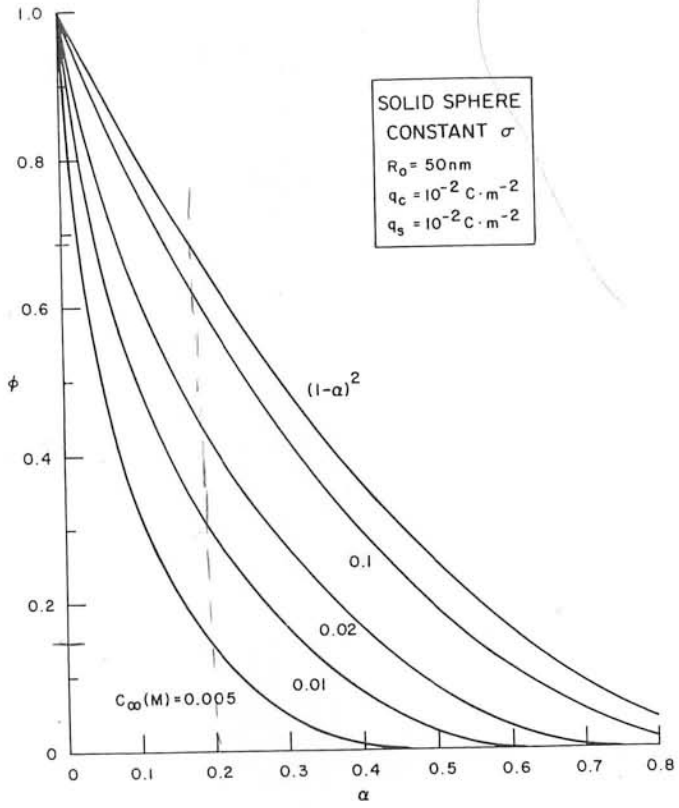

FIG. 3. Partition coefficients Φ as a function of α for solid spheres at constant surface charge density in a 50-nm-radius pore. The calculations assume an aqueous solution of a 1:1 univalent electrolyte at 37°C and the indicated molarities.

is given in Fig. 4. Here the partition coefficient is shown as a function of solution ionic strength, or the dimensionless parameter τ (pore radius/Debye length) for three values of the relative sphere size. The calculations for the solid sphere assume a fixed surface charge density of 10^{-2} C · m^{-2}. For each value of α the corresponding porous sphere volumetric charge density has been calculated to give the identical number of elementary charges in the two models, and the limiting case of unit porosity has been used. The porous sphere model (upper curves marked by P) shows less electrostatic interaction than the solid sphere model (marked by S) at all values of τ. That is, distributing the charge throughout the sphere volume gives a weaker electrostatic interaction with the pore wall than if that same charge resided on the sphere surface. For both models, at small values of τ, electrostatic effects are sufficient to virtually exclude all of the solute particles from the pore ($\Phi \rightarrow 0$). For large values of τ, the electrostatic interactions become unimportant and each curve approaches an asymptotic limit corresponding to purely steric exclusion, $\Phi \rightarrow (1 - \alpha)^2$, indicated with the dashed lines at each α. Variation in solution ionic strength (or τ) affects the solute equilibrium partitioning over a wide range of values. The square root scale required to convert from τ to electrolyte concentration should be noted.

Porous sphere models similar to that developed here have been used previously to represent randomly coiled polyelectrolytes in

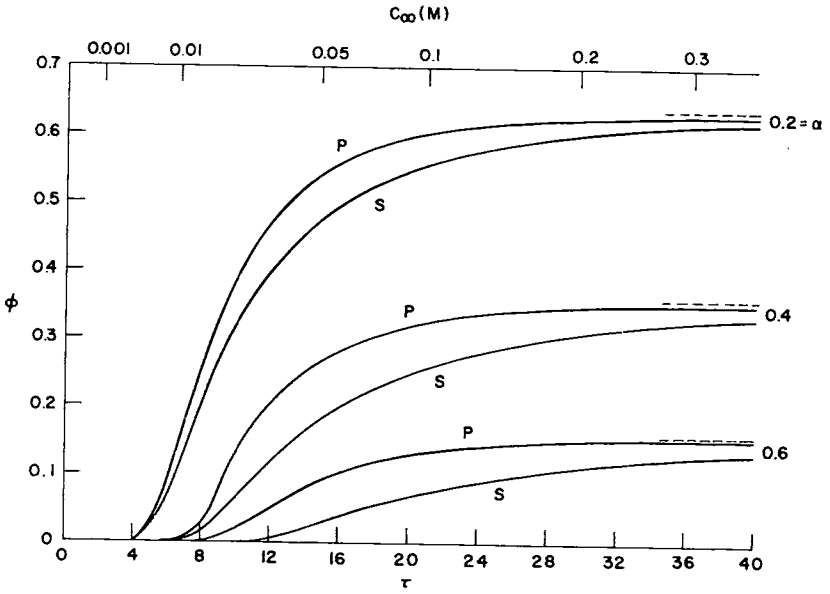

FIG. 4. Partition coefficient Φ as a function of τ or C_∞ for completely porous (P) and solid (S) spheres of identical size and total charge. Parameter values in the calculation are: R_0 = 20 nm, $q_c = 10^{-2}$ C·m^{-2}, $q_s = 10^{-2}$ C·m^{-2}, and an aqueous solution of a 1:1 univalent electrolyte at 37°C. The porous sphere charge density is calculated as $q_v = 3q_s/\alpha R_0$ to maintain equal particle charges. The dashed lines indicate asymptotic values approached at high ionic strength for each α.

solution (8, 9), with the sphere porosity, the volume fraction of solvent within the sphere, generally taken to be near unity. We found that varying the sphere porosity from 1.0 to 0.1 (at fixed dielectric constant ratio, $\bar{\delta} = 1.0$) did not appreciably alter the calculated partition coefficients. At a porosity of 0.01 some significant effects were observed, but such a low porosity indicates that the sphere might more correctly be modeled as a solid particle. It was also found that simultaneously adjusting the sphere dielectric constant ratio $\bar{\delta}$ with the porosity did not substantially change the results. The difficulty of estimating these parameters in any practical application and their minor impact on the calculated partition coefficients indicates that assuming $\bar{\delta}$ = 1 and γ = 1 is a useful simplification. Therefore, calculations for the porous sphere model in most instances may be performed using Eq. [38] in place of Eq. [37]. It may be noted that, with the solid sphere model, the sphere–solvent dielectric constant ratio does not enter the calculations in the first-order approximations, Eqs. [29] and [33].

The effect of varying the pore wall charge density on partition coefficient calculations is shown in Fig. 5. As expected, an increase in the surface charge density increases the electrostatic interaction and therefore decreases the value of the partition coefficient. The calculations predict significant electrostatic effects at relatively low values of the charge density. Of particular interest is the appearance of an electrostatic interaction even when the cylinder wall is uncharged. An inspection of Eqs. [29], [33], and [37] reveals a quadratic dependence of the interaction potentials on the surface charge density or the surface potential of both the sphere and the cylinder. The electrostatic interaction will then vanish if both surfaces are neutral but not if only one species is uncharged. This effect may be attributed to a distortion of the one existing double layer (sphere or cylinder) upon introducing the sphere into the pore.

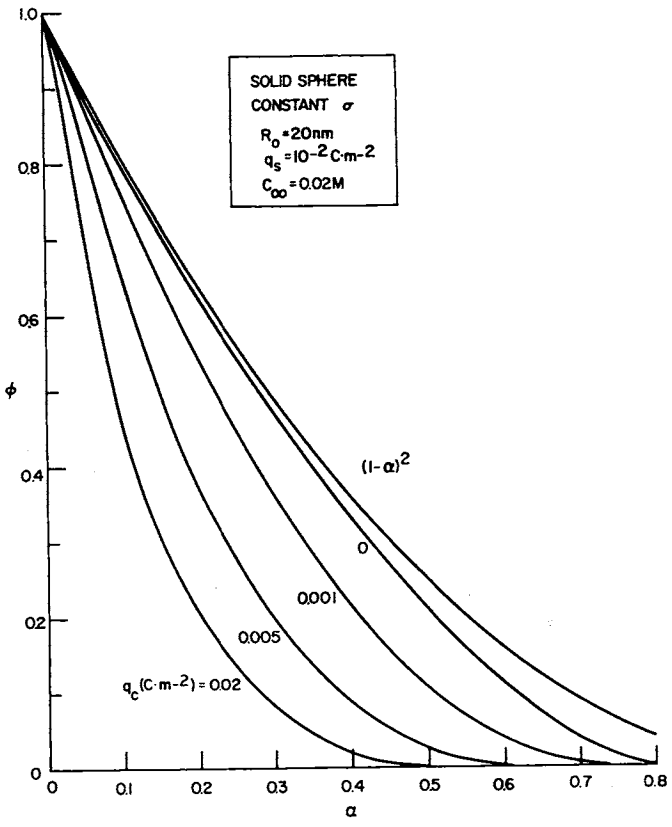

FIG. 5. Partition coefficient Φ as a function of α for solid spheres at constant surface charge density, for several values of the pore surface charge density q_c. The calculations assume an aqueous solution of a 1:1 univalent electrolyte at 37°C.

The electric field present is then required to satisfy different boundary conditions and hence the system free energy is altered even when only one double layer exists. This behavior is analogous to the dielectric exclusion effect discussed by Bean (10) in considering the transport of isolated charged particles in neutral pores. The exception is the uncharged, completely porous sphere, where no distortion of the cylinder double layer is required; the interaction energy vanishes for $\omega = 0$ in this case (Eq. [38]). With the parameter values assumed here, variation of the sphere surface charge density produces results nearly identical to those obtained in Fig. 5 from changes in the pore wall charge.

The results presented thus far have been calculated for interactions at constant charge densities between spheres and pores having charges of like sign. The interaction potential has always been a positive quantity, implying a repulsive force and giving partition coefficients less than the neutral values. Eqs. [29], [37], and [38] indicate that, if the charges are of like sign, electrostatic interactions at constant charge density will always be repulsive. For interaction at constant surface potential, the calculated values of Φ are generally only slightly greater than those obtained at constant charge, and the partition coefficients approach the constant charge values as $\alpha \rightarrow 1$ or as τ becomes large. However, at low solution ionic strength and for small values of α quite different behavior is observed. Figure 6 compares the partition coefficients obtained at $C_\infty = 0.005\ M$ for interactions

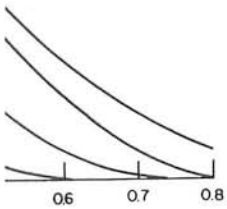

)heres at constant surface charge density,
lculations assume an aqueous solution of

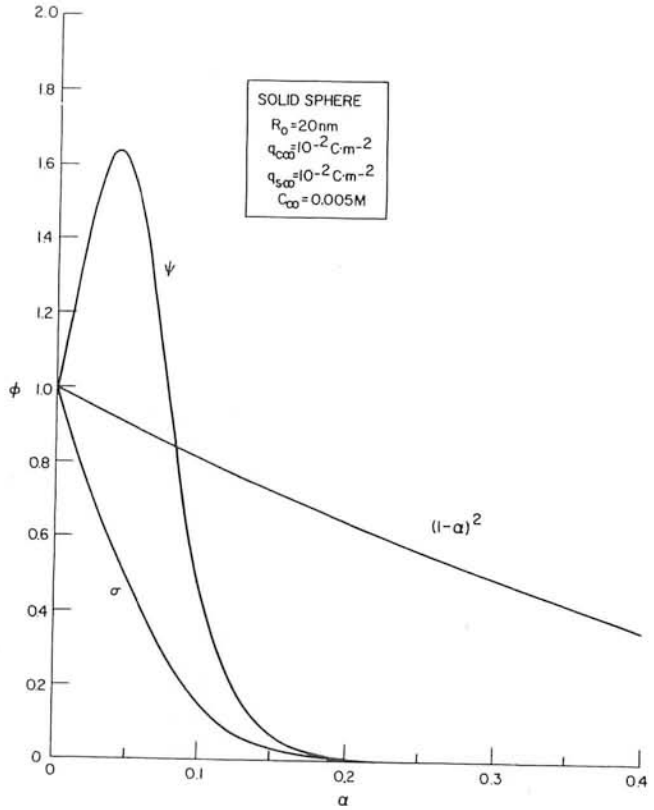

FIG. 6. A comparison of partition coefficients Φ as functions of α for solid spheres at constant surface charge density (σ) and constant surface potential (Ψ), at low ionic strength. The calculations assume an aqueous solution of a 1:1 univalent electrolyte at 37°C and identical surface charges at infinite separation.

es between spheres and pores having
; of like sign. The interaction potential
'ays been a positive quantity, implying
lsive force and giving partition coef-
; less than the neutral values. Eqs. [29],
ıd [38] indicate that, if the charges are
sign, electrostatic interactions at con-
harge density will always be repulsive.
eraction at constant surface potential,
culated values of Φ are generally only
/ greater than those obtained at con-
harge, and the partition coefficients
ıch the constant charge values as
or as τ becomes large. However, at
lution ionic strength and for small val-
α quite different behavior is observed.
6 compares the partition coefficients
ed at $C_\infty = 0.005\ M$ for interactions at constant surface charge density and constant surface potential. Not only do the constant potential results significantly exceed the fixed charge values for $\alpha < 0.15$ but partition coefficients greater than unity are predicted for $\alpha < 0.075$. Such behavior can be anticipated from the form of Eq. [33], where for some combinations of the parameter values, the negative terms in the numerator, containing the charge densities squared, may dominate over the positive term involving the cross product of the charge densities. If this occurs, a negative value for the interaction potential, indicating a double-layer attraction, will result for surface potentials of like sign. When this attractive force is strong enough over a portion of the pore cross section, integration of Eq. [1] can produce a partition coefficient greater than unity.

Effects similar to that observed in Fig. 6 are well recognized in the colloid literature. An early discussion is that given by Derjaguin (11) in an analysis of the coagulation of colloid particles of dissimilar size and charge. More current treatments and reviews are provided by Bell and Peterson (12) and by Usui (13). The explanation offered for these phenomena is as follows. As the two surfaces approach each other with the electrical potentials held constant, the surface charges must vary. That is, the potential gradient at each surface (or the equivalent surface charge density) must readjust in value to satisfy the constant potential boundary condition. In some cases, this readjustment

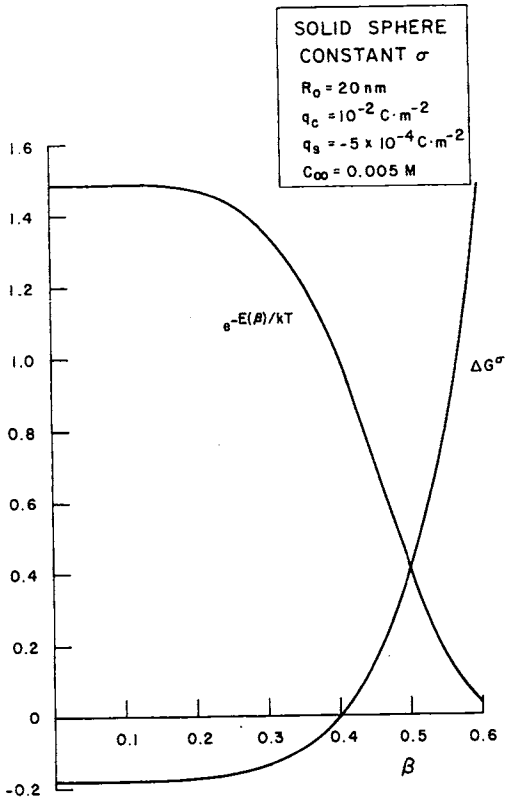

FIG. 7. Boltzmann factor and dimensionless interaction potential ΔG^σ as functions of β for solid sphere–pore interactions with constant surface charge densities of opposite sign. The calculations assume an aqueous solution of a 1:1 univalent electrolyte at 37°C and a sphere radius of 8 nm.

may reverse the sign of the charge on the surface of lower potential in an area around the point of closest approach. If this occurs, the surfaces may then experience an attractive interaction. Those parts of the surfaces where the double layers do not strongly interact or overlap may retain an electric charge of the original sign. Thus the total surface charge may remain of the same sign but be reduced in magnitude (14). These effects have been demonstrated clearly in the geometrically simple system of two plane parallel double layers interacting at constant surface potential or charge density (15–17). The references cited above (11, 13) show that this phenomenon occurs with the nonlinear Poisson–Boltzmann equation as well.

Exactly analogous arguments may be applied to interactions at constant surface charge densities to explain apparent repulsive behavior between oppositely charged surfaces. As Eqs. [29], [37], and [38] show, it is possible to choose parameter values such that a positive interaction potential will result. Again, if the terms involving the squares of the charge densities dominate the calculation, such a result can occur. This indicates a reversal in the sign of the surface potential within an area on one surface during the interaction.

An example of the effects just discussed for oppositely charged surfaces interacting at constant surface charge densities is shown in Fig. 7. The interaction potential calculated from Eq. [29] and the corresponding Boltzmann exponential factor are plotted here as a function of radial position for an 8-nm sphere in a 20-nm pore (α = 0.4) at a low ionic strength. A change in the interaction potential from an attractive (negative) quantity near the pore centerline to a repulsive (positive) value near the wall is observed. As the interaction potential changes sign, the exponential factor changes from values greater than one to values below unity. The Boltzmann exponential is directly related to the probability of finding a sphere at radial position β, and indicates the average sphere concentration at each radial position within the pore compared to the value in the external bulk solution. It is interesting to note that the particle concentration is relatively uniform near the center of the pore at a value approximately 1.48 times that in bulk solution. The concentration, however, decreases rapidly in the vicinity of the pore wall so that, when the exponential factor is radially averaged over the pore cross section, a partition coefficient of 0.30 is obtained. This is less than the neutral value of 0.36. For neutral surfaces, the sphere concentration would be unity between the centerline and β = 0.6.

Additional calculations of partition coefficients for oppositely charged double layers interacting at constant surface charge density

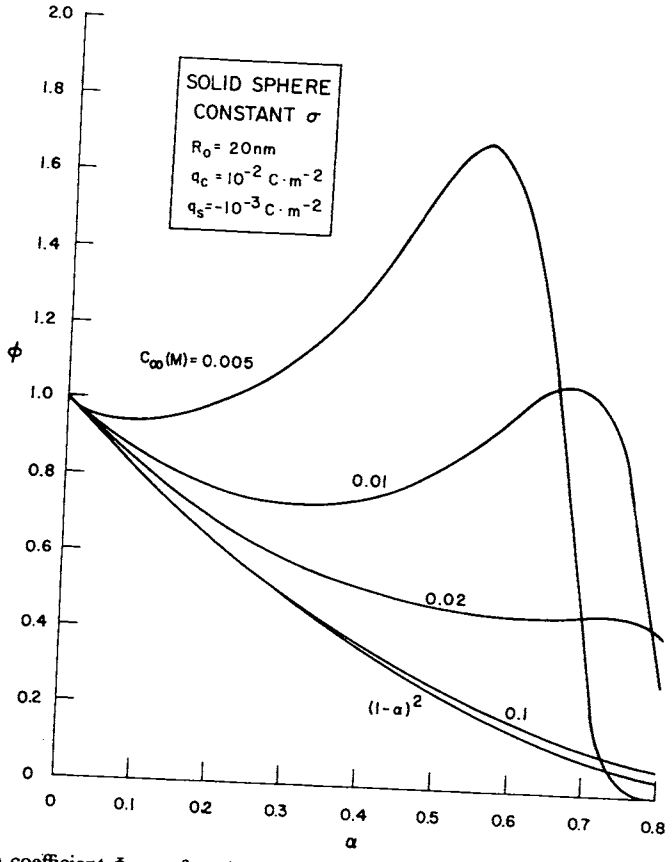

FIG. 8. Partition coefficient Φ as a function of α for solid spheres at constant surface charge density interacting with a pore having a surface charge of the opposite sign. The calculations assume an aqueous solution of a 1:1 univalent electrolyte at 37°C and the indicated molarities.

are presented in Fig. 8. The complex shape of the $\Phi(\alpha)$ curves may be explained as follows. Initially, at small values of α, steric exclusion is the dominant factor and the partition coefficients decrease as the sphere size increases. The attractive electrostatic interaction causes the partition coefficient values to exceed the neutral results and this electrostatic effect increases with decreasing ionic strength. As the relative particle size increases, double-layer interaction becomes more important and the curves attain a positive slope, eventually reaching a local maximum value. At this point steric effects, perhaps coupled with a change in sign of one of the surface potentials, become dominant and the partition coefficients decrease rapidly with increasing particle size. That the curves cross each other at large α and, at 0.005 M ionic strength, even fall below the neutral curve indicates that the net electrostatic interaction has become repulsive as discussed above.

As demonstrated by the calculations in Fig. 8, a slight opposite charge on one surface can produce significant net electrostatic effects. At somewhat larger charge densities (e.g., $q_s = -10^{-2}$ C·m^{-2}) the interaction potential became a large negative number and the exponential factor rapidly increased. Partition coefficients calculated under these conditions were unreasonably large, and the dilute solution theory employed here is likely then to be invalidated.

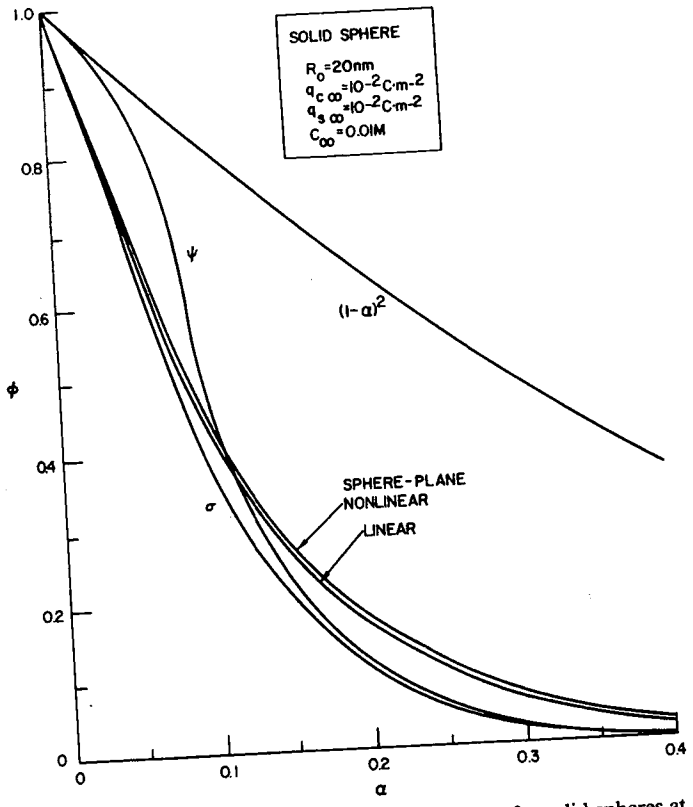

FIG. 9. A comparison of partition coefficients Φ as functions of α for solid spheres at constant surface charge density (σ) and constant surface potential (Ψ) with corresponding results for linear (Eq. [41]) and nonlinear (Eq. [40]) sphere–plane interactions. The calculations assume an aqueous solution of a 1:1 univalent electrolyte at 37°C.

Finally, it is informative to compare the present treatment of electrostatic effects on partitioning with approximate treatments employed previously (2, 3, 18, 19). In our earlier study (3) reporting results for the axisymmetric case only, it was necessary in integrating Eq. [1] to assume a functional form for the radial dependence of E. This was taken to be $E(\beta) = E(0)\exp(\tau\beta)$, based on findings for repulsive interactions between planar surfaces (15) and between a sphere and a plane surface (14). From Eqs. [29], [30], [33], [37], and [38] it is now apparent that E varies more nearly as $I_0(\tau\beta)$. For similar parameter values, in a plot such as Fig. 4, the former assumption of an exponential variation causes Φ to approach its asymptotic value somewhat more slowly than the present results as τ is increased.

Several other investigators (2, 18, 19) have performed sphere–pore interaction calculations using a relation derived by Bell *et al.* (14), which is strictly valid only for the interaction between a sphere and a plane. Additional restrictions on this result, which is based on the nonlinear Poisson–Boltzmann equation, are that the charged surfaces must be separated by at least two Debye lengths, and that the sphere radius must be relatively large (more than about five Debye lengths). Although the derivation assumes constant surface potentials, similar results would be obtained for constant charge boundary conditions, given the large separations required.

Converted to the interaction potential form and to the present notation, the sphere–plane result becomes

$$\Delta G^{\Psi} = 64\pi\alpha \tanh\left(\frac{\Psi_s}{4}\right) \tanh\left(\frac{\Psi_c}{4}\right) \times e^{-\tau(1-\alpha)} e^{\tau\beta}. \quad [40]$$

The corresponding linearized form is

$$\Delta G^{\Psi} = 4\pi\alpha\Psi_s\Psi_c e^{-\tau(1-\alpha)} e^{\tau\beta}. \quad [41]$$

A detailed analysis of the relationship between these equations and the theoretical results derived here is given elsewhere (5).

Partition coefficients calculated from both the nonlinear (Eq. [40]) and linear (Eq. [41]) sphere–plane equations are compared in Fig. 9 to values obtained with the more rigorous sphere–pore theory reported here. Values of the more exact partition coefficients obtained for interaction at both constant charge density and constant surface potential are included. For the parameter values tested, the results are in surprisingly close agreement. As might be expected from an approximation neglecting wall curvature, the sphere–plane solution generally underestimates the electrostatic interaction effect. This approximation is also unable to reproduce the crossover in the interaction potential from repulsive to attractive behavior, discussed above. This phenomenon increases the more exact partition coefficients at constant surface potential significantly for small α, where deviation from the sphere–plane approximation becomes greatest. The relatively small difference between results obtained using the linear and nonlinear forms of this approximation is a consequence of the surface potentials not exceeding 50 mV in these constant potential calculations.

Use of the linearized form of the Poisson–Boltzmann equation, Eq. [3], has allowed us to obtain analytical expressions for the desired interaction energies. Interaction energies calculated using the linear and non-linear equations have been compared for two planar surfaces (20) or two spheres (16), and the results found to be similar for plane surface potentials as high as 100 mV and sphere surface potentials as high as 50 mV. Our parameter values were chosen so that specified surface potentials did not exceed 70 mV, so that we would not expect our calculated results to be changed markedly if the nonlinear equation were used, at least in the constant potential cases. For repulsive interactions at constant surface charge, surface potentials may become very large at small enough separations between the sphere and pore surfaces. In such instances, with $E > 0$, there again may be little difference between partition coefficients calculated using the linear and nonlinear equations, since the exponential factor in Eq. [1] will tend to vanish in either case at close separations. As already noted, it is probably unreasonable to model strong attractive interactions ($E \ll 0$) with the present theory, since the underlying assumption of vanishingly small particle concentration in the pore may be readily invalidated as pore-to-bulk solution partition coefficients become large.

ACKNOWLEDGMENT

This work was supported by Grant ENG-7905576 from the National Science Foundation.

REFERENCES

1. Brenner, H., and Gaydos, L. J., *J. Colloid Interface Sci.* **58,** 312 (1977).
2. Malone, D. M., and Anderson, J. L., *Chem. Eng. Sci.* **33,** 1429 (1978).
3. Smith III, F. G., and Deen, W. M., *J. Colloid Interface Sci.* **78,** 444 (1980).
4. Verwey, E. J. W., and Overbeek, J. Th. G., "Theory of the Stability of Lyophobic Colloids." Elsevier, Amsterdam, 1948.
5. Smith III, F. G., "Electrostatic Effects on the Restricted Diffusion of Macromolecules." Sc.D. thesis, Massachusetts Institute of Technology, August, 1981.
6. Eyges, L., "The Classical Electromagnetic Field." Addison–Wesley, Reading, MA, 1972.
7. Karasz, F. E., and Hill, T. L., *Arch. Biochem. Biophys.* **97,** 505 (1962).

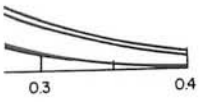

α for solid spheres at constant surface
nding results for linear (Eq. [41]) and
assume an aqueous solution of a 1:1

iewhat more slowly than the pres-
s as τ is increased.
other investigators (2, 18, 19) have
d sphere–pore interaction calcula-
ıg a relation derived by Bell *et al.*
ch is strictly valid only for the in-
between a sphere and a plane. Ad-
estrictions on this result, which is
the nonlinear Poisson–Boltzmann
, are that the charged surfaces must
ated by at least two Debye lengths,
the sphere radius must be relatively
ore than about five Debye lengths).
ı the derivation assumes constant
potentials, similar results would be
l for constant charge boundary con-
given the large separations required.

8. Tanford, C., "Physical Chemistry of Macromolecules." Wiley, New York, 1961.
9. Hermans, J. J., and Overbeek, J. Th. G., *Rec. Trav. Chim.* **67,** 761 (1948).
10. Bean, C. P., *in* "Membranes—A Series of Advances" (G. Eisenman, Ed.), Vol. 1, pp. 1–54. Dekker, New York, 1972.
11. Derjaguin, B. V., *Discuss. Faraday Soc.* **18,** 85 (1954).
12. Bell, G. M., and Peterson, G. C., *J. Colloid Interface Sci.* **41,** 542 (1972).
13. Usui, S., *in* "Progress in Surface and Membrane Science" (J. F. Danielli, M. D. Rosenberg, and D. A. Cadenhead, Eds.), Vol. 5, pp. 223–266. Academic Press, New York, 1972.
14. Bell, G. M., Levine, S., and McCartney, L. N., *J. Colloid Interface Sci.* **33,** 335 (1970).
15. Usui, S., *J. Colloid Interface Sci.* **44,** 107 (1973).
16. Kar, G., Chander, S., and Mika, T. S., *J. Colloid Interface Sci.* **44,** 347 (1973).
17. Parsegian, V. A., and Gingell, D., *Biophys. J.* **12,** 1192 (1972).
18. Prieve, D. C., and Hoysan, P. M., *J. Colloid Interface Sci.* **64,** 201 (1978).
19. Silebi, C. A., and McHugh, A. J., *AIChE J.* **24,** 204 (1978).
20. Hogg, R., Healy, T. W., and Fuerstenau, D. W., *Trans. Faraday Soc.* **62,** 1638 (1966).

$$\tau = \frac{\text{pure rad}}{\lambda_D} \qquad \text{n.d.}$$

$$\alpha = \frac{R_s}{R_p} \qquad \text{n.d.}$$

$$\beta = \frac{x}{R_p} \qquad \text{n.d.} \quad 0 \ldots 1$$

$$\Psi = \frac{F \phi^*}{RT} \qquad \text{n.d.}$$